Developmental Biology 445 (2019) 103–112

Contents lists available at ScienceDirect

Developmental Biology

journal homepage: www.elsevier.com/locate/developmentalbiology

Original research article

Essential role of mouse Dead end1 in the maintenance of spermatogonia

Yuki Niimi[a], Atsuki Imai[a], Hitomi Nishimura[a], Kenya Yui[a], Ai Kikuchi[a], Hiroko Koike[c], Yumiko Saga[c], Atsushi Suzuki[a,b,*]

[a] Division of Materials Science and Chemical Engineering, Graduate School of Engineering, Yokohama National University, Yokohama, Kanagawa 240-8501, Japan
[b] Division of Materials Science and Chemical Engineering, Faculty of Engineering, Yokohama National University, Yokohama, Kanagawa 240-8501, Japan
[c] Division of Mammalian Development, National Institute of Genetics, Mishima, Shizuoka 411-8540, Japan

ARTICLE INFO

Keywords:
Testis
Spermatogenesis
Spermatogonia
Stem cell

ABSTRACT

Dead end is a vertebrate-specific RNA-binding protein implicated in germ cell development. We have previously shown that mouse Dead end1 (DND1) is expressed in male embryonic germ cells and directly interacts with NANOS2 to cooperatively promote sexual differentiation of fetal germ cells. In addition, we have also reported that NANOS2 is expressed in self-renewing spermatogonial stem cells and is required for the maintenance of the stem cell state. However, it remains to be determined whether DND1 works with NANOS2 in the spermatogonia. Here, we show that DND1 is expressed in a subpopulation of differentiating spermatogonia and undifferentiated spermatogonia, including NANOS2-positive spermatogonia. Conditional disruption of DND1 depleted both differentiating and undifferentiated spermatogonia; however, the numbers of A_{single} and A_{paired} spermatogonia were preferentially decreased as compared with those of $A_{aligned}$ spermatogonia. Finally, we found that postnatal DND1 associates with NANOS2 *in vivo*, independently of RNA, and interacts with some of NANOS2-target mRNAs. These data not only suggest that DND1 is a partner of NANOS2 in undifferentiated spermatogonia as well as in male embryonic germ cells, but also show that DND1 plays an essential role in the survival of differentiating spermatogonia.

1. Introduction

Mammalian testes continuously produce a huge number of sperm cells throughout life. This reproductive characteristic is maintained by a robust stem cell system comprising the spermatogonial stem cell (SSC) population. In mouse testes, SSC function resides in a subfraction of undifferentiated spermatogonial cells, which consist of A_{single} (A_s; isolated spermatogonia), A_{paired} (A_{pr}; 2 cell chains) and $A_{aligned}$ (A_{al}; chains with 4 or more cells) (de Rooij, 1998, 2001). These cells give rise to differentiating spermatogonia, which undergo additional divisions and then enter a meiotic pathway. Although various genes expressed specifically in undifferentiated spermatogonia have been reported (Buaas et al., 2004; Costoya et al., 2004; Oatley et al., 2011; Suzuki et al., 2009; Tokuda et al., 2007; Yoshida et al., 2004; Zheng et al., 2009), the factors contributing to SSC functions are not fully elucidated; thus, the molecular basis of stemness remains elusive. Recently, we have reported that most A_s and A_{pr} undifferentiated spermatogonia express the RNA-binding protein NANOS2, which is essential for sexual differentiation of fetal male germ cells, and that this protein is required for adult SSC self-renewal during steady-state spermatogenesis (Sada et al., 2009; Suzuki and Saga, 2008; Suzuki et al., 2009). Therefore, NANOS2 is considered key to understanding SSC stemness.

Dead end is an RNA-binding protein initially identified as an essential factor for germ cell development in zebrafish (Weidinger et al., 2003). The mouse homologue, Dead end1 is encoded by *Dnd1*, to which the spontaneous mutation, *Ter*, was recently mapped. In the *Ter* mutation, a single cytosine in the third exon of *Dnd1* is changed to thymine, which generates a premature stop codon, resulting in a null mutation of *Dnd1* by nonsense-mediated mRNA decay (Youngren et al., 2005). Although the homozygous mutant mice grew into seemingly normal adults, over 90% of the male mutant 129/Sv mice developed testicular teratomas originated from primordial germ cells (Stevens, 1967, 1973). In other mouse strains, *Ter*-homo adult males show complete sterility, while female mice possess a small number of oocytes and show subfertility owing to a reduction in the number of primordial germ cells during embryogenesis (Noguchi and Noguchi, 1985). These findings suggest a distinctive role for DND1 in male germ cell development. We have previously shown that DND1 interacts with NANOS2 in male embryonic germ cells for the recruitment of specific

* Corresponding author at: Division of Materials Science and Chemical Engineering, Faculty of Engineering, Yokohama National University, Yokohama, Kanagawa, Japan.
E-mail address: suzuki-atsushi-gz@ynu.ac.jp (A. Suzuki).

https://doi.org/10.1016/j.ydbio.2018.11.003
Received 19 July 2018; Received in revised form 8 November 2018; Accepted 8 November 2018
Available online 12 November 2018

RNAs to the CCR4-NOT deadenylase complex (CNOT complex), leading them to the degradation pathway (Suzuki et al., 2010, 2016). Thus, DND1 cooperatively functions with NANOS2 during the sexual differentiation of male embryonic germ cells; this raises the question of whether DND1 is also expressed in undifferentiated spermatogonia and acts as a partner of NANOS2 to maintain these cells.

In the current study, we attempted to elucidate DND1 functions during spermatogenesis, especially focusing on the relationship with NANOS2. We found that DND1 is expressed in differentiating and undifferentiated spermatogonia including NANOS2-expressing cells, and that the proteins interact with each other in spermatogonia. Additionally, we aimed to examine the physiological role of DND1 in spermatogonia *in vivo*, establishing a *Dnd1*-conditional knockout (*Dnd1*-cKO) mouse strain.

2. Materials and methods

2.1. Ethics statement

Animal experiments were carried out with the permission of the animal experimental committee at Yokohama National University and the National Institute of Genetics.

2.2. Mice

Dnd1-flox, Rosa-CreER^{T2}, and transgenic mice expressing Flag-tagged DND1 have been previously described (Suzuki et al., 2016). Both of the *Dnd1*-flox mice and the Rosa-CreER^{T2} mice have been backcrossed onto a MCH(ICR) hybrid strain (CLEA Japan, Inc.) for 8 generations. NANOS2-O/E mice have also been described previously (Sada et al., 2009). In brief, *CAG-CAT-3×FLAG-Nanos2* transgenic mice were crossed with *Nanos3*-Cre mice (Suzuki et al., 2008) to induce forced expression of Flag-tagged NANOS2 in germ cells.

2.3. Western blotting

100 mg of various tissues indicated in Figs. 1A and 2B were homogenized in 1 ml of 1× sample buffer, boiled and then spun at 17,000 × *g* for 10 min at 25 °C. The supernatants were separated by SDS-PAGE and analyzed according to the standard procedure.

2.4. Histological methods

For histological analysis, testes were fixed with Bouin's solution overnight, embedded in paraffin, and then sectioned at 6 μm. After deparaffinization, the sections were stained with hematoxylin and eosin according to the standard procedure.

2.5. Immunostaining

For section immunostaining of DND1, NANOS2, and PLZF, adult testes were fixed with 4% paraformaldehyde (PFA) overnight, embedded in paraffin, and sectioned at 6 μm. After deparaffinization, the sections were autoclaved for 15 min at 121 °C with Antigen Unmasking Solution (Vector Laboratories, CA, USA) followed by blocking with 5% skim milk for 30 min, and then incubated overnight at 4 °C with primary antibodies against DND1 (1: 2000) produced by a guinea pig (Suzuki et al., 2016), NANOS2 (1: 100) (Sada et al., 2009; Suzuki and Saga, 2008), or PLZF (1: 2000; H-300; Santa Cruz Biotechnology).

For whole-mount immunostaining, untangled seminiferous tubules were prepared as previously described (Nakagawa et al., 2010) with slight modifications. Adult mouse testes were removed from the tunica albuginea and fixed with 4% PFA for 1 h at 4 °C. The samples were attached to MAS-coated slide glass (Matsunami, Osaka, Japan) by half-drying. After incubation in 0.1% Tween-20 in PBS [PBS-T] for 10 min, the samples were dehydrated through a methanol series (25%, 50%, 75%, and 100% in PBS containing 0.1% Tween-20 [PBS-T]) on ice, followed by rehydration in PBS-T. For immunostaining of DND1, NANOS2, NANOS3, or PLZF, the samples were autoclaved for 15 min at 121 °C with Antigen Unmasking Solution (Vector Laboratories, CA, USA) followed by blocking with 5% skim milk in PBS for 1 h, and then incubated overnight at 4 °C with primary antibodies against DND1 (1: 2000), NANOS2 (1: 100), NANOS3 (1: 800), or PLZF (1: 2000; H-300; Santa Cruz Biotechnology, USA). For immunostaining of GFRα1, CDH1, c-KIT, or TEX14, the samples were directly treated with 5% skim milk in PBS for 1 h without autoclaving, and then incubated overnight at 4 °C with antibodies against GFRα1 (1:200; R & D Systems, MN, USA), CDH1 (1: 800; 13–1900; Invitrogen, CA, USA), c-KIT (1: 500; a gift from Dr. Hirata, (Yamatani et al., 2004)), or TEX14 (1: 3200; a gift from Dr. Iwamori).

After washing, the section and samples were incubated with Alexa 355-, Alexa 488- or Alexa 594-conjugated IgG antibody (1: 500; Life Technologies, CA, USA) for 2 h at 25 °C, enclosed in Fluoromount™ (Diagnostic Biosystems, CA, USA), and then observed using fluorescence microscopy (AxioImager.M2; Carl Zeiss, Germany).

All antibodies used were diluted with Can Get Signal immunoreaction enhancer solution (Toyobo, Osaka, Japan).

2.6. Flow cytometry

Testis cell suspensions were generated by sequential digest of dissected and minced seminiferous tubules with 1 mg/ml collagenase (Wako, Japan) and then 0.25% Trypsin (27250018, Thermo Fisher Scientific, USA) containing 1 mM EDTA. Cells were passed through a 40-μm strainer to remove clumps. Harvested cells were resuspended in HBSS containing 5% FBS and 0.1% BSA for subsequent staining. The following antibodies to cell surface markers were used: c-KIT (1: 100; a gift from Dr. Hirata, (Yamatani et al., 2004)), APC anti-TER119 (BD Bioscience, NJ, USA), and APC anti-CD45 (BD Bioscience, NJ, USA). Ter119 antibody and CD45 antibody were used to remove autofluorescence by blood cells. Anti-c-KIT antibody was detected using Alexa 594-conjugated anti-Armenian Hamster IgG antibody (Life Technologies, CA, USA). For combination of intracellular staining of DAZL, PLZF or SOHLH1, FoxP3 Transcription Factor Staining Buffer Kit (A25866A, Life Technologies, CA, USA) were used with antibodies against DAZL (1: 500) produced by a guinea pig (Suzuki et al., 2016), PLZF (1: 200; H-300; Santa Cruz Biotechnology, USA) and SOHLH1 (1: 100; a gift from Dr. Rajkovic) according to manufacturer's instructions. DNA was labelled with DAPI to gate 2 N and 4 N fractions. Stained cells were analyzed on a Cell Sorter (MoFlo Astrios, BeckmanCoulter, CA, USA).

2.7. Tamoxifen treatment

Tamoxifen (Sigma, T5648) was dissolved in sesame oil (Sigma, S3547) at 20 mg/ml in a light-blocking tube at 55 °C. After filtration, the solution was administered intraperitoneally to mice at 75 mg/kg body weight for 5 consecutive days.

2.8. Immunoprecipitation and western blotting

For the immunoprecipitation of DND1 and NANOS2, 100 mg of testes from 8-week-old wild-type mice were homogenized on ice in 1 ml of Buffer A (25 mM HEPES-KOH [pH 7.4], 250 mM sucrose, 75 mM β-glycerophosphate, 1 mM DTT, 0.05% NP-40, 1 mM PMSF) with 400 units/ml RNase inhibitor (Toyobo, Osaka, Japan) or 100 μg/ml RNase A (Sigma, MO, USA), and spun at 10,000 × *g* for 10 min at 4 °C. NaCl (5 M) was then added to the supernatants to a final concentration of 150 mM. The samples were mixed with 20 μl of Protein A Sepharose CL-4B (GE Healthcare) crosslinked with guinea pig anti-DND1 antibody (Suzuki et al., 2016), normal guinea pig IgG (MBL, Nagoya, Japan), rabbit anti-NANOS2 antibody, or rabbit preimmune serum by

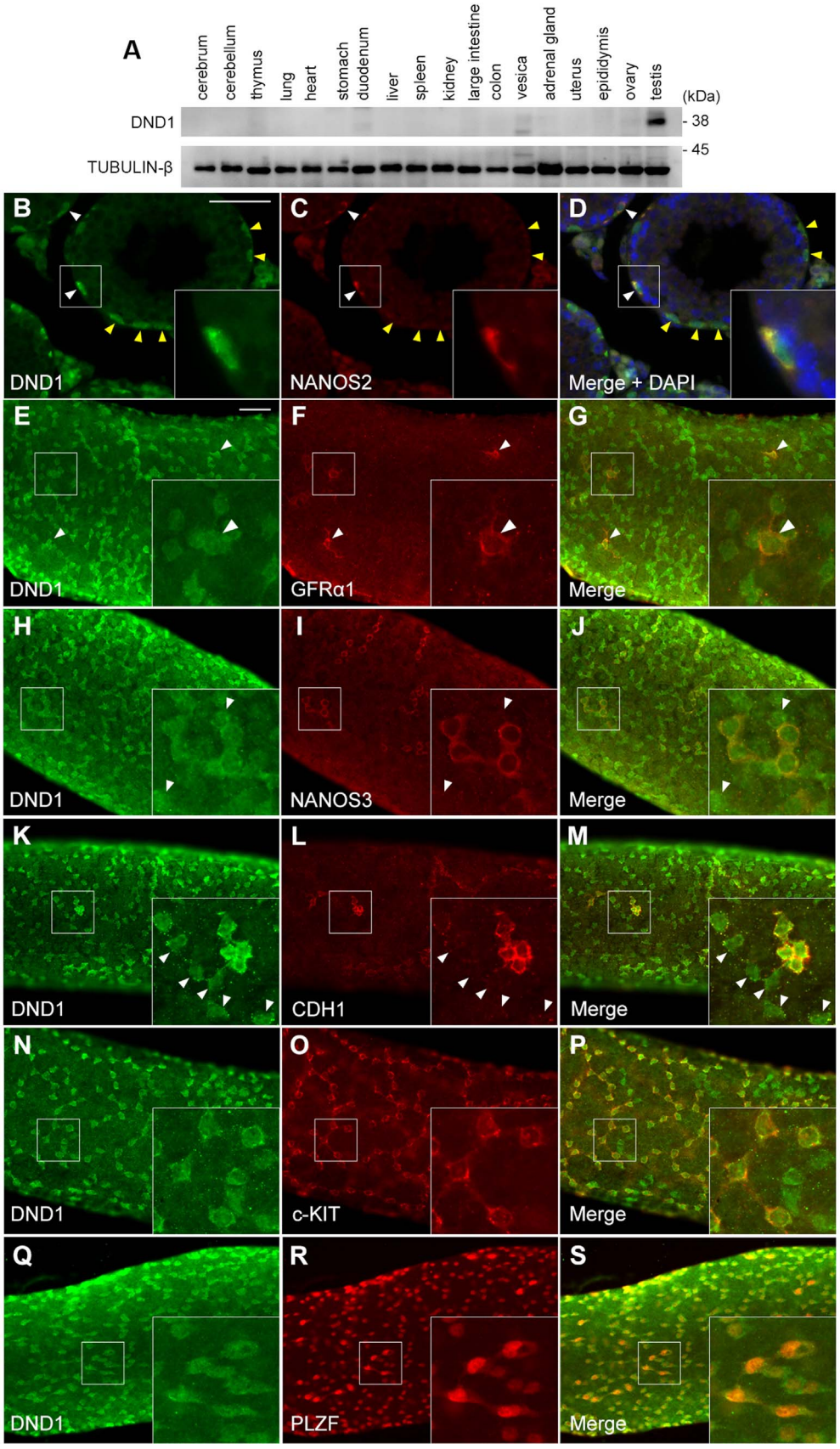

Fig. 1. Expression profile of DND1 in adult mouse testes. A, Western blot analyses of DND1 protein in various tissues from 5-week-old mice. TUBULIN-β was used as a loading control. **B–D,** Testis sections of a 6-week-old mouse were immunostained with antibodies against DND1 (green) (**B**) and NANOS2 (red) (**C**). DNA was labelled with DAPI (blue) (**D**). White arrowheads indicate cells expressing both DND1 and NANOS2, whereas yellow arrowheads indicate cells expressing DND1 alone. **E–S,** Whole-mount immunostaining of seminiferous tubules of a 6-week-old mouse with antibodies against DND1 (green) (**E, H, K, N, Q**), GFRα1 (red) (**F**), NANOS3 (**I**), CDH1 (**L**), c-KIT (**O**), and PLZF (**R**). Arrowheads in **E–G** indicate co-expression of DND1 and GFRα1, whereas arrowheads in **H–J** and **K–M** indicate DND1-positive NANOS3-negative cells (**H–J**) and DND1-positive CDH1-negative cells (**K–M**), respectively; scale bars: 50 μm in **B** for **B–D, E** for **E–S.** Insets in **B–S** show enlarged views to better visualize protein expression.

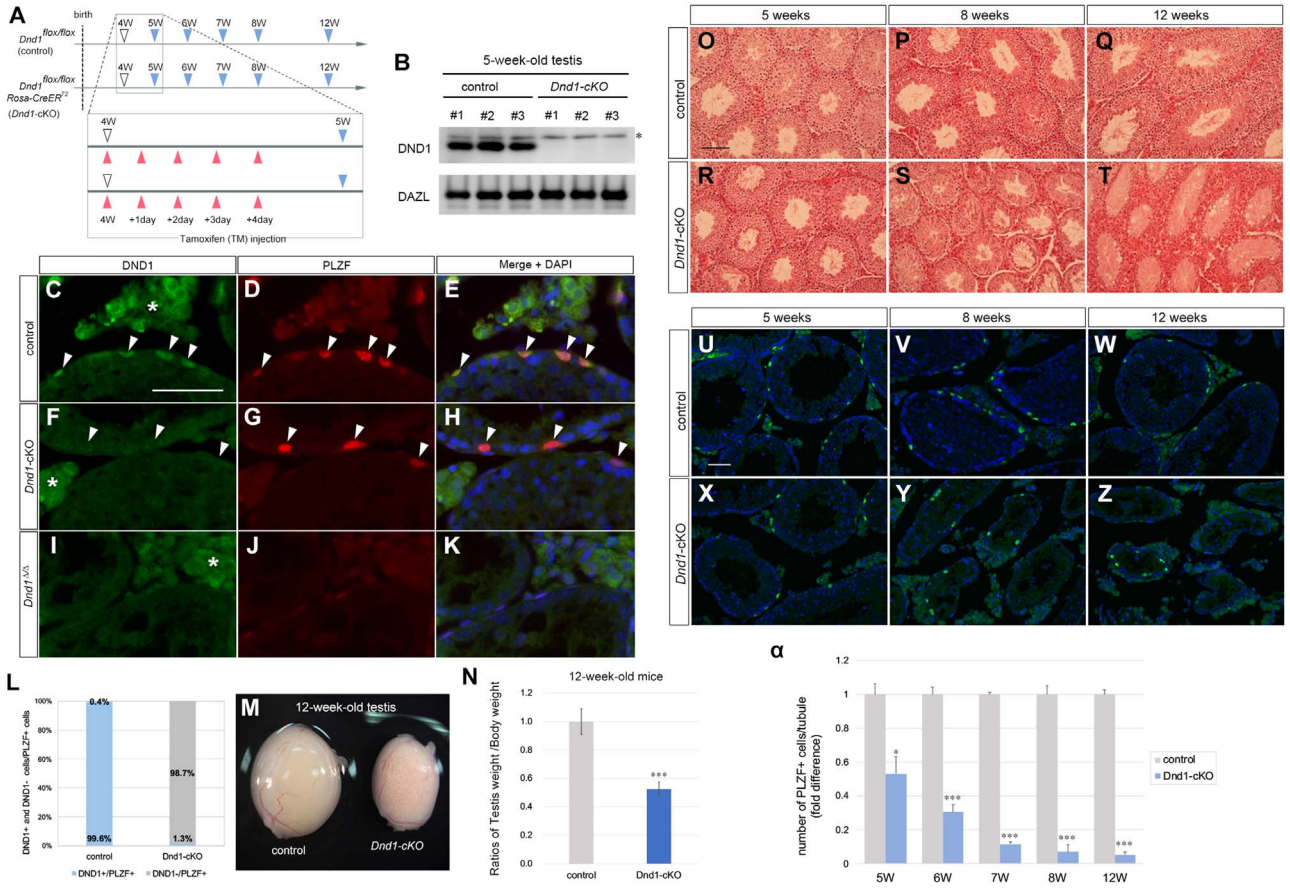

Fig. 2. Conditional knockout of *Dnd1* causes depletion of PLZF-positive spermatogonia. A, Schematic representation of experimental strategy: for conditional knockout of postnatal DND1, TM was injected into both 4-week-old *Dnd1*$^{flox/flox}$ (control) mice and *Dnd1*$^{flox/flox}$; *Rosa-CreER*^{T2} (*Dnd1*-cKO) mice for 5 consecutive days (red arrowheads), and the testes from these mice were harvested at the indicated time points (blue arrowheads). **B,** Western blot analysis of DND1 protein in 5-week-old testes from control and *Dnd1*-cKO mice; three mice per genotype were analyzed (#1, #2, and #3). DAZL was used as a loading control. An asterisk indicate non-specific signals. **C–K,** Testis sections of 5-week-old control, *Dnd1*-cKO, and *Dnd1*-null (*Dnd1*$^{\Delta/\Delta}$) mice were immunostained with antibodies against DND1 (green) (**C, F, I**) and PLZF (red) (**D, G, J**). DNA was labelled with DAPI (**E, H, K**). Asterisks in **C**, **F**, and **I** indicate non-specific signals in somatic cells. Arrowheads in **C**–**H** indicate cells positive for PLZF. Note that *Dnd1*-null testis sections serve as the negative control for immunostaining. **L,** Ratios of the numbers of DND1-positive cells and DND1-negative cells per the number of PLZF-positive cells were calculated by counting each cell in section immunostaining of DND1 and PLZF; 100 tubules from more than 10 independent microscopic fields were scored ($n = 3$). **M,** Comparison of testis size in 12-week-old littermates from control and *Dnd1*-cKO mice. **N,** Testis weight per Body weight ratios of 12-week-old control and *Dnd1*-cKO mice. The results were normalized using those of control mice. Error bars represent mean ± SD; three mice per genotype were analyzed. *** $P < 0.001$ (Student's *t*-test). **O–T,** Testis sections of 5-, 8-, and 12-week-old control and *Dnd1*-cKO mice were stained with hematoxylin and eosin. **U–Z,** Testis sections of 5-, 8-, and 12-week-old control and *Dnd1*-cKO mice were immunostained with an anti-PLZF antibody. DNA was labelled with DAPI (blue). **α,** Number of PLZF-positive spermatogonia per seminiferous tubule in sections. More than 100 tubules from 20 independent microscopic fields were scored ($n = 3$). The results were normalized using the corresponding control for each stage. Scale bars: 50 μm in **C** for **C–K**, **O** for **O–T**, **U** for **U–Z**.

disuccinimidyl suberate (Pierce Biotechnology, IL, USA) on a rotator for 3 h at 4 °C. After 10 washes with Buffer A containing 150 mM NaCl, the sepharose was boiled in 20 μl of 2 × sample buffer.

For immunoprecipitation of Flag-tagged DND1 and NANOS2, testis extracts were generated from 6-week-old *Dnd1*-heterozygous mice, *Dnd1*-null mice with the transgene, or *CAG-CAT-3×FLAG-Nanos2/Nanos3*-Cre mice as mentioned above. The samples were then incubated with 50 μl of anti-FLAG M2 affinity gel (A2220, Sigma, MO, USA) or mouse IgG-agarose (A0919, Sigma, MO, USA) on a rotator for 3 h at 4 °C. After 5 washes with Buffer A containing 150 mM NaCl, precipitates were eluted with 500 μg/ml of 3×FLAG peptides in Buffer A containing 150 mM NaCl on a rotator for 1 h at 25 °C and then concentrated using methanol and chloroform.

The samples were subjected to SDS-PAGE and analyzed by western blotting with antibodies against DND1 (1: 800), NANOS3 (1: 800), NANOS2 (1: 800), CNOT1 (1: 500, provided by H. T. Timmers), CNOT3 (1: 500, provided by T. Tamura), CNOT9 (1: 500, provided by H. Okayama).

2.9. Immunoprecipitation and RT-qPCR

Flag-tagged DND1 or NANOS2 was immunoprecipitated from testes extracts as mentioned above. After elution of precipitates by 3× FLAG peptides, co-precipitated RNAs were purified using TRIzol® Reagent (Life Technologies, CA, USA) and used for first-strand cDNA synthesis with 200 U SuperScript III reverse transcriptase (Invitrogen) and 100 pmol $(dT)_{20}$ primer (Invitrogen). Quantitative PCR was performed on the Thermal Cycler Dice® Real Time System (Takara Bio, Shiga, Japan) using SYBR® *Premix Ex Taq*™ II (Tli RNaseH plus) (Takara Bio, Shiga, Japan) in 20-μl reactions. For qPCR with *Sohlh1* and *Sohlh2* primers, the reaction was held at 98 °C for 1 min followed by 45 cycles of 98 °C for 10 s, 62 °C for 20 s, and 72 °C for 30 s. For qPCR with other primers, the reaction was held at 94 °C for 1 min followed by 45 cycles of 94 °C for 30 s, 60 °C for 30 s, and 72 °C for 45 s. Each sample was analyzed in triplicate, and three biological replicates ($n = 3$) were included, and the relative amounts of transcripts was calculated by the standard curve method using Multiple RQ Software (Takara Bio, Shiga, Japan). The level of *Actinβ* control mRNA was used to normalize mRNA levels of target genes. For the RNAs co-precipitated with Flag-tagged DND1, the fold enrichment of each mRNA in

immunoprecipitates (IP) from *Dnd1*-null testes extracts with the transgene (Δ/Δ + *tg*) compared to IP from *Dnd1*- heterozygous testes extracts (+/Δ) was calculated (ratio of each mRNA level in FLAG IP from *tg* to those from *wt*). For the RNAs co-precipitated with Flag-tagged NANOS2, the fold enrichment of each mRNA in immunoprecipitates (IP) of anti-FLAG M2 affinity gel (α-FLAG, A2220, Sigma, MO, USA) compared with IP of Mouse IgG-Agarose (IgG, A0919, Sigma, MO, USA) was calculated (ratio of each mRNA level in FLAG IP to IgG IP).

2.10. Primers

Primer pairs used for the RT-qPCR analyses were as follows:

Ddx4-Fw: 5′-GCTTCATCAGATATTGGCGAGT-3′ and
Ddx4-Rv: 5′-GCTTGGAAAACCCTCTGCTT-3′ for *Ddx4* (NM_001145885.1).
Dmrt1-Fw: 5′-CTGGAAACCAGTGGCAGATG-3′ and
Dmrt1-Rv: 5′-GCGAGAACACACTGGCTTTG-3′ for *Dmrt1* (NM_015826.5).
Sohlh1-Fw: 5′-AGCCAGACTCCGGTATAGCCA-3′ and
Sohlh1-Rv: 5′-CAAGCTGGAAGACTCTGGCT-3′ for *Sohlh1* (NM_001001714.1).
Sohlh2-Fw: 5′-CTTTGGAGGGAGCAGTGAGAG-3′ and
Sohlh2-Rv: 5′-GTGCAGTGGGTGGCAAATAAG-3′ for *Sohlh2* (NM_028937.3).
Dazl-Fw: 5′-CTATTCTGTCAGGATTGCTC-3′ and
Dazl-Rv: 5′-CAGTTGTGATATGACCCATT-3′ for *Dazl* (NM_010021.5).
Taf7l-Fw: 5′-GAGGGACAGAAGTATGTGGT-3′ and
Taf7l-Rv: 5′-TTTAGCCTCCATGAAGCAGA-3′ for *Taf7l* (NM_028958.4).
Actinβ-Fw: 5′-AAAGACCTCTATGCCAACAC-3′ and
Actinβ-Rv: 5′-TGCTTGCTGATCCACATCTG-3′ for *Actinβ* (NM_007393.5).

2.11. Statistical analysis

The statistical significance of differences in cell numbers, ratios of testis weight per body weight, ratios in flow cytometry, and RT-qPCR analysis results was assessed using a two-tailed *t*-test. A P-value < 0.05 was considered to represent statistical significance. Statistical analysis was conducted using Microsoft Excel.

3. Results

3.1. DND1 expression profile in adult testes

The Mouse ENCODE transcriptome data show that *Dnd1* mRNA is expressed in various adult tissues. However, the protein expression of DND1 still remains obscure. We have previously generated specific antibodies against DND1, and confirmed its expression in male embryonic germ cells by western blotting and immunostaining (Suzuki et al., 2016). Therefore, we examined DND1 expression in various tissues of adult mice by western blotting using the antibody, and found a strong signal of DND1 only in the testis, suggesting DND1 functions during spermatogenesis (Fig. 1A).

We next aimed to identify DND1-expressing cells in adult testes and examined whether DND1 is co-expressed with NANOS2 in these cells. Section immunostaining revealed strong signals of DND1 in both the nucleus and cytoplasm in a fraction of cells on the basement membrane of seminiferous tubules (Fig. 1B). In addition, some of them were positive for NANOS2 expression (Fig. 1B–D, white arrowheads). We have counted the number of DND1-positive cells per NANOS2-positive cells and found that more than 99.8% of NANOS2-positive cells expressed DND1 (Fig. S1A), suggesting that DND1 is expressed in undifferentiated spermatogonia. To clarify the expression profile of DND1 in detail, we examined glial cell line-derived neurotrophic factor family receptor alpha 1 (GFRα1), because this protein is expressed preferentially in A_s and A_{pr} undifferentiated spermatogonia during steady-state spermatogenesis, similar to NANOS2 (Grasso et al., 2012; Sada et al., 2009), while many of aligned A-type spermatogonia become GFRα1-positive in regenerative response to busulfan treatment (Chan et al., 2017; Nakagawa et al., 2010). Double-immunostaining analyses of whole seminiferous tubules revealed the expression of GFRα1 in a subpopulation of DND1-positive cells (Fig. 1E–G and Fig. S1B), confirming that DND1-expressing cells include A_s and A_{pr} undifferentiated spermatogonia. We then compared the DND1-positive cell population with that positive for NANOS3, which associates with DND1 *in vitro* and is expressed in A_{al} undifferentiated spermatogonia (Suzuki et al., 2016, 2009). Immunostaining analyses revealed that DND1 is expressed in all the NANOS3-positive undifferentiated spermatogonia (Fig. 1H–J and Fig. S1C), although the staining signals were also observed in NANOS3-negative spermatogonia (Fig. 1H–J, arrowheads). Therefore, we next compared DND1 expression with that of cadherin 1 (CDH1), a marker for all undifferentiated spermatogonia from A_s to $A_{al>16}$ (Tokuda et al., 2007). Immunostaining analyses revealed that almost all CDH1-positive undifferentiated spermatogonia expressed DND1 (Fig. 1K–M and Fig. S1D), as expected. These data indicate that DND1 is expressed in all the populations of undifferentiated spermatogonia. However, the CDH1 expression was very weak in some of DND1-positive cells (Fig. 1K–M, arrowheads), suggesting that DND1 is also expressed in differentiating spermatogonia. To determine the point at which DND1 expression ends during differentiation of spermatogonia, the expression of c-KIT, a marker for spermatogonia differentiating into early spermatocytes (Schrans-Stassen et al., 1999; Yoshinaga et al., 1991), was analyzed with DND1. Whole-mount immunostaining analyses of seminiferous tubules showed that a portion of DND1-positive undifferentiated spermatogonia co-expressed c-KIT (Fig. 1N–P), and that the ratio of c-KIT positive cells gradually increased with increase in cluster cell number of undifferentiated spermatogonia (Fig. S1E). After differentiation of undifferentiated spermatogonia, the expression of DND1 was weakly detected in all c-KIT-positive differentiating spermatogonia at Stage IV of the seminiferous epithelial cycle (Fig. S1G, H). However, its expression was gradually downregulated in association with the differentiation of spermatogonia; this expression finally disappeared in more differentiated spermatogonia at Stage V (Fig. S1G, I). Collectively, these findings indicate that DND1 is expressed in all populations of undifferentiated spermatogonia and a part of differentiating spermatogonia from A1 to at least through A3 spermatogonia, which is very similar to the expression profile of promyelocytic leukemia zinc-finger (PLZF) (Buaas et al., 2004; Costoya et al., 2004; Suzuki et al., 2009). Therefore, we then compared the DND1 expression with that of PLZF, and found almost complete co-localization of DND1 and PLZF signals (Fig. 1Q–S, Fig. 2L, and Fig. S1J).

3.2. Conditional deletion of Dnd1 causes spermatogenic defects

To address the physiological role of DND1 during spermatogenesis, we crossed *Dnd1*-flox mice (Suzuki et al., 2016) with *Rosa-CreER*^{T2} mice, and administered tamoxifen (TM) pulses to both 4-week-old *Dnd1*$^{flox/flox}$ (control) and *Dnd1*$^{flox/flox}$*; Rosa-CreER*^{T2} (*Dnd1*-conditional knockout; *Dnd1*-cKO) mice for 5 consecutive days to delete *Dnd1* in a whole-body manner (Fig. 2A). We first examined the deletion of *Dnd1* from genomic DNA of PLZF-positive spermatogonia isolated from the 5-week-old control and *Dnd1*-cKO testes (Fig. S2A). PCR analyses revealed the Cre-mediated recombination of loxP sequence in the PLZF-positive spermatogonia (Fig. S2B, C). We then examined the expression of DND1 in the 5-week-old *Dnd1*-cKO testes by western blotting and found that the signal of DND1 was depleted (Fig. 2B). Section immunostaining analyses showed that DND1 ex-

pression was removed from PLZF-positive spermatogonia in the 5-week-old *Dnd1*-cKO testes (Fig. 2C–K). To quantitate the deletion efficiency, we counted DND1-positive and DND1-negative cells per PLZF-positive cells and found that the DND1 protein was expressed in 99.6% of PLZF-positive cells; however, this was depleted to 1.3% as of 1 week after the first pulse of TM (Fig. 2L), These data indicate that DND1 was almost completely depleted from PLZF-positive spermatogonia during 1 week after first injection of TM.

We then measured the body weights of 12-week-old control and *Dnd1*-cKO mice to assess the physiological effect of TM injection and *Dnd1* deletion, and found no significant change (Fig. S3), suggesting that neither TM injection nor *Dnd1* deletion had a deleterious effect on somatic tissues. On the other hand, the testis size in *Dnd1*-cKO mice was decreased as compared with those in control mice during 8 weeks after TM pulses (Fig. 2M); testis weight was approximately 50% lower than that in control mice (Fig. 2N). Histological analyses revealed that the number of germ cells progressively declined with age after TM pulses (Fig. 2O–T), resulting in sterility of these mice. To determine the cause of germ-cell loss observed in *Dnd1*-cKO mice, we analyzed PLZF-positive spermatogonia during the 12 weeks after TM administration by section-immunostaining with an anti-PLZF antibody. PLZF-positive cells in the testes of *Dnd1*-cKO mice seemed morphologically unchanged; however, the numbers were obviously lower at 8 and 12 weeks compared with that in control testes (Fig. 2U–Z). We then counted the number of PLZF-positive cells and found that the number gradually declined with age, resulting in almost half of the number of control testes even within 1 week after TM injection in the absence of DND1 (Fig. 2α, 5W). These data indicate that the spermatogenic defects in *Dnd1*-cKO testes are caused by loss of spermatogonia.

3.3. Both differentiating and undifferentiated spermatogonia are decreased in Dnd1-cKO mice

To assess the primary defect caused by the deletion of DND1, we next aimed to examine the each population of differentiating and undifferentiated spermatogonia in the testes of 5-week-old *Dnd1*-cKO mice. For this purpose, cells in the testes from 5-week-old control and *Dnd1*-cKO mice were subjected to flow cytometric analysis using antibodies against DAZL and PLZF (Fig. 3A, B, gate D). These analyses revealed that the number of PLZF-positive cells was decreased to about half in the absence of DND1 (Fig. 3C), confirming the result in Fig. 2α. Then, we analyzed the population of spermatogonia double-positive for PLZF and c-KIT in the testes of control and *Dnd1*-cKO mice (Fig. 3D, E, gate D), since DND1 is expressed in a part of c-KIT-positive differentiating spermatogonia (Fig. S1G). Flow cytometric analyses revealed that PLZF- and c-KIT-positive cells were decreased in the absence of DND1 (Fig. 3F), suggesting a reduction of the differentiating spermatogonia. Therefore, we further examined the SOHLH1-positive cell population because SOHLH1 is mainly expressed in c-KIT-positive spermatogonia (Suzuki et al., 2012), and found that the population of SOHLH1- and c-KIT-positive spermatogonia (Fig. 3G, H, gate D) was clearly decreased to less than one-third in *Dnd1*-cKO testes as expected (Fig. 3I). To identify the cause of the reduction of these cells in *Dnd1*-cKO testes, we examined whether these cells undergo apoptotic cell death using antibodies against cleaved Caspase 3 (active-Casp3) and c-KIT (Fig. 3J–O). Section immunostaining analyses showed that the active-Casp3 signal was significantly upregulated in c-KIT-positive cells in *Dnd1*-cKO testes (Fig. 3P), suggesting that the c-KIT-positive differentiating spermatogonia undergo apoptotic cell death in the absence of DND1. From these data, DND1 is essential for the survival of differentiating spermatogonia.

On the other hand, flow cytometric analyses also revealed that the number of c-KIT-negative and PLZF-positive undifferentiated spermatogonia significantly decreased in the absence of DND1 (Fig. 3D, E, gate E, and Q). To determine the population of undifferentiated spermatogonia decreased in *Dnd1*-cKO testes, we conducted whole-mount immunostaining of seminiferous tubules with antibodies against GFRα1 and PLZF (Fig. 4A–F); then, the numbers of double-positive cell clusters were counted as A_s, A_{pr}, A_{al-4} and A_{al-8} (Fig. 4G). These analyses revealed that the cluster numbers of A_s and A_{pr} spermatogonia were significantly decreased in *Dnd1*-cKO testes, while the A_{al-4} and A_{al-8} clusters seemed unchanged. However, since GFRα1 might be expressed only in a part of the A_{al-4} and A_{al-8} spermatogonia, we performed further immunostaining using antibodies against CDH1 and PLZF to count the cluster number of aligned spermatogonia in more detail. In addition, an antibody against TEX14 was also used to visualize the cell connections in the clusters (Iwamori et al., 2012) (Fig. 4H–M). These analyses showed that the numbers of A_s and A_{pr} clusters were decreased as in the case of GFRα1 in *Dnd1*-cKO mice as anticipated. On the other hand, we were surprised to find that the cluster number of A_{al-4} was slightly but significantly increased, while the A_{al-8} and A_{al-16} clusters were unchanged (Fig. 4N). Although the cause of these changes of spermatogonial cluster number are unclear because apoptotic cell death was not observed in A_s and A_{pr} spermatogonia even in the absence of DND1 (Fig. S4), these data at least indicate that DND1 functions reside in undifferentiated spermatogonia, especially in A_s and A_{pr} clusters, in which NANOS2 is mainly expressed.

3.4. DND1 interacts with NANOS2 and some of its target RNAs in spermatogonia

In adult *Nanos2*-cKO mouse testes, germ cells are gradually lost because of depletion of spermatogonial stem cells (Sada et al., 2009). As DND1 cooperatively functions with NANOS2 in male embryonic germ cells (Suzuki et al., 2016), we presumed that DND1 also partners with NANOS2 for the maintenance of A_s and A_{pr} undifferentiated spermatogonia. To test this hypothesis, we assessed the interaction between DND1 and NANOS2 in postnatal testes. Immunoprecipitation analyses revealed that the antibody against DND1 efficiently precipitated DND1 from testis extracts, although the amount was larger in the presence of RNase than in the absence (Fig. 5A). This may be because disruption of DND1-RNA complex exposed the accessible surface of DND1 for the antibody used, resulting in more efficient precipitation. Under this condition, a small amount of NANOS2 was co-precipitated in addition to NANOS3 as expected. However, the signals were very faint, possibly owing to the small number of NANOS2-expressing cells in whole testes and even in DND1-expressing spermatogonia. Therefore, we carried out a reciprocal immunoprecipitation using antibody against NANOS2, and found co-precipitation of DND1 in addition to the components of CCR4-NOT deadenylase complex, CNOT1, CNOT3, and CNOT9 (Fig. 5B), which were shown to interacts with NANOS2 (Bhandari et al., 2014; Suzuki et al., 2010). These results indicate that there is an interaction between DND1 and NANOS2 in spermatogonia as well as in male embryonic germ cells.

We further examined whether DND1 associates with NANOS2-interacting RNAs in spermatogonia. Although our antibody is able to precipitate NANOS2 from testis extracts, the amount is too small to analyze its interacting RNAs. To overcome these difficulties, we took advantage of a transgenic mouse line, in which Flag-tagged NANOS2 is over-expressed by Cre-loxP system specifically in germ cells (Sada et al., 2009). In the testes of NANOS2-overexpressing (O/E) mice, seminiferous tubules are filled with Flag-tagged NANOS2-positive spermatogonia because differentiation is strongly repressed (Sada et al., 2009), which allows us to carry out biochemical analyses of NANOS2. We first conducted immunoprecipitation of Flag-tagged NANOS2 from testis extracts of the NANOS2-O/E mice with anti-Flag antibody (Fig. 5C, Blue lines) and found clear co-precipitation of CNOT1, CNOT3, CNOT9, and DND1, regardless of RNase treatment (Fig. 5D), thus confirming the interaction with DND1. As NANOS2 has been shown to interact with mRNAs of *Sohlh1*, *Sohlh2*, *Dmrt1*, *Taf7l*, and *Dazl* genes, but not *Ddx4* mRNA in germline stem cells (Zhou

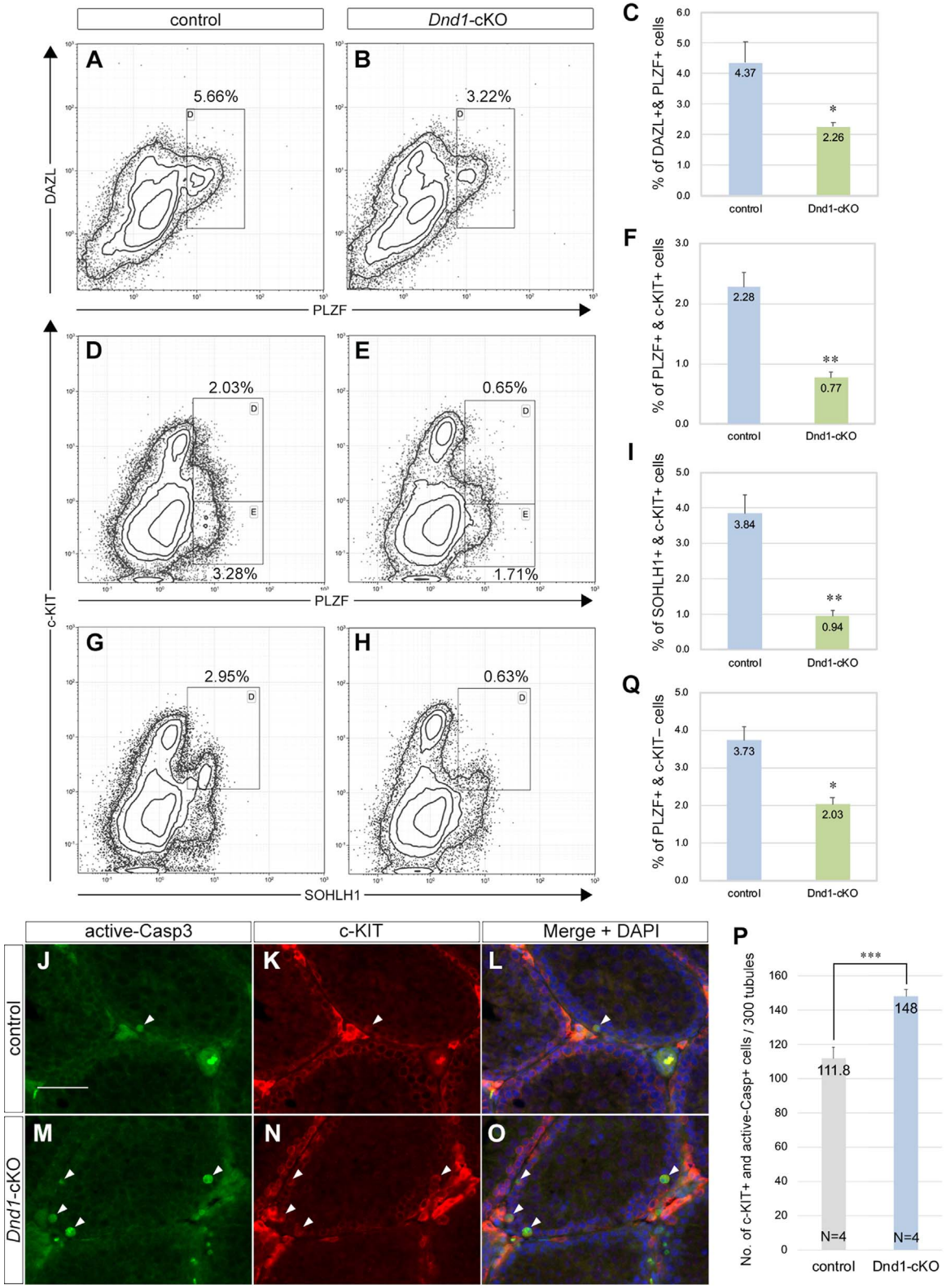

Fig. 3. Differentiating spermatogonia decrease in *Dnd1*-cKO testes. A–I, Flow cytometric analyses of testis cells from 5-week-old control (**A, D, G**) and *Dnd1*-cKO (**B, E, H**) mice using antibodies against PLZF and DAZL (**A, B**), PLZF and c-KIT (**D, E**), or SOHLH1 and c-KIT (**G, H**). Percentages of cells within each gate are indicated. Frequency of indicated cell fractions among testis cells of PLZF+ and DAZL+ (**C**), PLZF+ and c-KIT+ (**F**), or SOHLH1+ and c-KIT+ (**I**) were determined by the flow cytometric analyses. * $P < 0.05$, ** $P < 0.01$. Error bars in **C, F** and **I** represent mean SD; three mice per genotype were analyzed. **J–O,** Testis sections from 5-week-old control and *Dnd1*-cKO mice were immunostained with antibodies against active-Casp3 (green) (**J, M**) and c-KIT (red) (**K, N**). DNA was labelled with DAPI (**L, O**). Arrowheads indicate cells double positive for active-Casp3 and c-KIT. **P,** Number of cells double positive for active-Casp3 and c-KIT in **J–O** were counted in 300 tubules from more than 20 independent microscopic fields ($n = 4$); *** $P < 0.001$ (Student's *t*-test); scale bar: 50 μm in **J** for **J–O. Q,** Frequency of indicated cell fractions among testis cells of PLZF+ and c-KIT– in **D** and **E** were determined by the flow cytometric analyses. * $P < 0.05$. Error bars represent mean SD; three mice per genotype were analyzed.

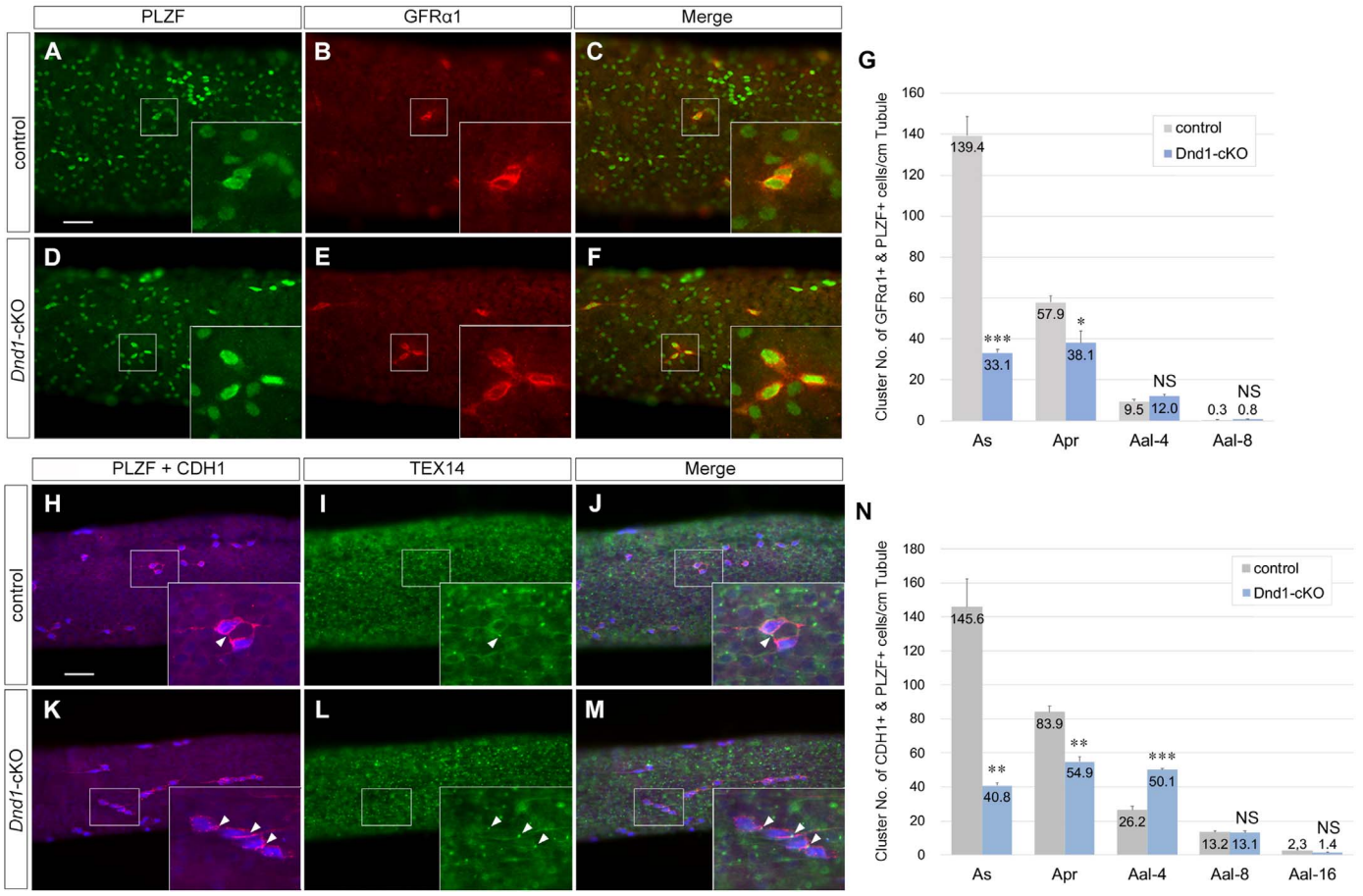

Fig. 4. A_s and A_{pr} spermatogonia decrease in *Dnd1*-cKO testes. A–F, Seminiferous tubules of 5-week-old control and *Dnd1*-cKO mice were immunostained with antibodies against PLZF (green) (**A, D**), GFRα1 (red) (**B, E**). **G,** Number of clusters double-positive for GFRα1 and PLZF in **A–F** were counted from undifferentiated A_s to $A_{al>8}$ spermatogonia per 1-cm tubule ($n = 3$). Clusters other than those of 2^n cells are omitted. **H–M,** Seminiferous tubules of 5-week-old control and *Dnd1*-cKO mice were immunostained with antibodies against PLZF (blue) (**H, K**), CDH1 (red) (**H, K**), and TEX14 (green) (**I, L**). **N,** Number of clusters double-positive for CDH1 and PLZF in **H–M** were counted from undifferentiated A_s to A_{al-16} spermatogonia per 1-cm tubule ($n = 4$). Clusters other than those of 2^n cells are omitted. * $P < 0.05$, *** $P < 0.001$ (Student's *t*-test); scale bars: 50 μm in **A** for **A–F, H** for **H–M.** Insets in **A–F** and **H–M** show enlarged views to better visualize protein expression. Arrowheads in **H–M** indicate localization of TEX14 to show cell connections in the clusters. Error bars in **G** and **N** represent mean SD.

et al., 2015), we then analyzed these mRNAs by immunoprecipitation of Flag-tagged NANOS2 and RT-qPCR (Fig. 5C, magenta lines). All the tested mRNAs, except *Ddx4* mRNA, were co-precipitated with Flag-tagged NANOS2 (Fig. 5E), indicating that the mRNAs are associated with NANOS2 *in vivo* as anticipated.

We then analyzed whether these mRNAs also associate with DND1. Because our antibody against DND1 is not very useful for precipitation of DND1-RNA complex (Fig. 5A), we took advantage of another transgenic mouse line expressing Flag-tagged DND1, which was previously reported to fully rescue the phenotype of *Ter*-homo mice (Suzuki et al., 2016). We introduced the transgene into *Dnd1*-null (*Dnd1*$^{\Delta/\Delta}$) mice and confirmed that the transgene also fully rescued the phenotype of *Dnd1*$^{\Delta/\Delta}$ mice (Fig. S5). Then, we carried out immunoprecipitation using the rescued testes (Fig. 5F, Blue lines). As expected, the antibody against Flag efficiently precipitated Flag-tagged DND1, resulting in the co-precipitation of NANOS2 and NANOS3 regardless of RNase treatment (Fig. 5G). Then, we conducted immunoprecipitation and RT-qPCR analyses (Fig. 5F, magenta lines) and found that all the NANOS2-associated mRNAs were precipitated with DND1, although the amount of the mRNAs co-precipitated was small (Fig. 5H). As the amount of NANOS2 co-precipitated with Flag-tagged DND1 was very small (Fig. 5G, α-NANOS2), the amount of NANOS2-interacting RNAs was also expected to be very small. Nevertheless, these data suggest that DND1 regulates the mRNAs cooperatively with NANOS2.

4. Discussion

In the current study, we found that both differentiating and undifferentiated spermatogonia were decreased by 1 week after the first pulse of TM in the *Dnd1*-cKO testes (Fig. 3A–I, Q). Among these two cell-types, undifferentiated spermatogonia showed a preferential reduction of A_s and A_{pr} spermatogonia (Fig. 4G, N), in which DND1 interacts with NANOS2 (Fig. 5A, B). Therefore, the observed reduction in spermatogonia may be attributed to the disruption of the DND1-NANOS2 complex. Considering that the apoptotic signal was not observed in GFRα1-positive undifferentiated spermatogonia (Fig. S4) while the number of A_{al-4} spermatogonial cluster was slightly increased (Fig. 4N), A_s and A_{pr} spermatogonia might be quickly divided into A_{al-4} spermatogonia without self-renewal by 1 week after the first TM pulse, which suggest that A_s and A_{pr} spermatogonia might fail to turnover at a normal rate of 6–7 days (de Rooij, 2017). Alternatively, it is also possible that some of A_s and A_{pr} spermatogonia directly differentiate into GFRα1-negative differentiating spermatogonia or meiotic cells in *Dnd1*-cKO testes, in a similar manner to that observed in male embryonic germ cells showing meiotic characters in the absence of DND1 (Suzuki et al., 2016). However, we currently lack evidence confirming either the mitotic division or the differentiation of these cells. Further analysis is required for elucidation of the status of A_s and A_{pr} undifferentiated spermatogonia in the absence of DND1. On the other hand, apoptotic cell death was significantly upregulated in the

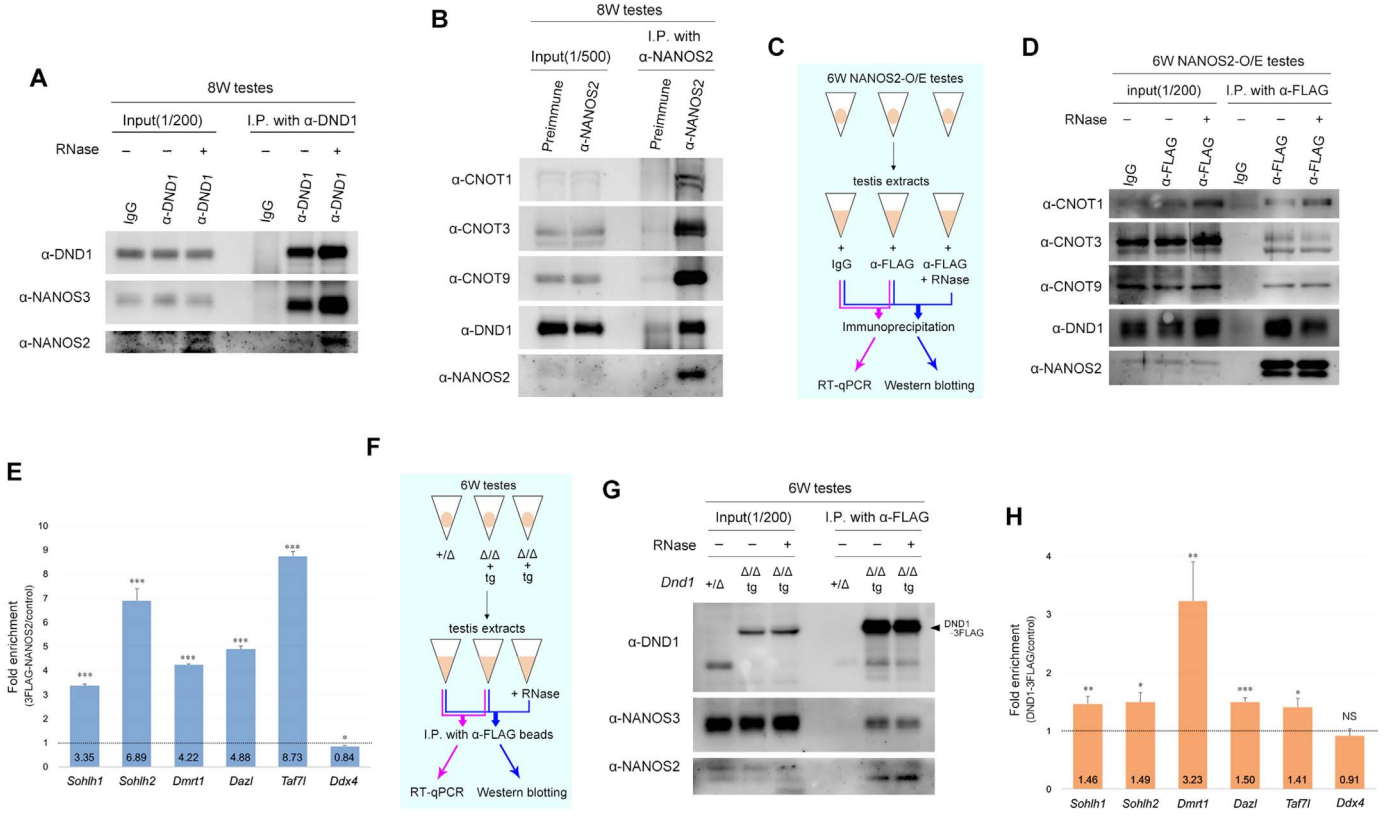

Fig. 5. DND1 associates with NANOS2 and some of its target RNAs in adult testes. A, Western blot analyses of proteins co-precipitated with anti-DND1 antibody from testis extracts of 8-week-old wild-type mice, with or without RNase. IgG was used as a negative control. **B,** Western blot analyses of proteins co-precipitated with anti-NANOS2 antibody from testis extracts of 8-week-old wild-type mice. Preimmune serum was used as a negative control. **C,** Schematic representation of IP experiments using testes from 6-week-old Flag-tagged NANOS2-O/E mice. **D,** Western blot analyses of proteins co-precipitated with anti-FLAG antibody from testis extracts of 6-week-old Flag-tagged NANOS2-O/E mice with or without RNase. IgG was used as a negative control. **E,** RT-qPCR analyses of mRNAs co-precipitated with anti-FLAG antibody from testis extracts of 6-week-old Flag-tagged NANOS2-O/E mice. **F,** Schematic representation of IP experiments using 6-week-old testes from *Dnd1*- heterozygous (+/Δ) mice and *Dnd1*-null mice with the transgene expressing Flag-tagged DND1 (Δ/Δ + tg). **G,** Western blot analyses of proteins co-precipitated with anti-FLAG antibody from testis extracts of 6-week-old *Dnd1*-heterozygous (+/Δ) mice and *Dnd1*-null mice with the transgene expressing Flag-tagged DND1 (Δ/Δ + tg) with or without RNase. **H,** RT-qPCR analyses of mRNAs co-precipitated with anti-FLAG antibody from testis extracts of 6-week-old *Dnd1*-heterozygous (+/Δ) mice and *Dnd1*-null mice with the transgene expressing Flag-tagged DND1 (Δ/Δ + tg). Quantitative RT-qPCR data in **E** and **H** are shown as average relative mRNA levels. Error bars represent mean SE ($n = 3$).

differentiating spermatogonia (Fig. 3P), accounting for the reduction of these cells. As DND1 is expressed in NANOS2-negative spermatogonia, DND1 might have some functions that are independent of NANOS2 in these cells; In fact, we found that NANOS3 interacts with DND1 in the adult testes. As NANOS3 is expressed mainly in NANOS2-negative undifferentiated spermatogonia (Sada et al., 2009), DND1 might have a cooperative function with NANOS3 instead of NANOS2 in these cells. Therefore, disruption of the DND1-NANOS3 complex might have some effects on NANOS2-negative undifferentiated spermatogonia, which may indirectly promote the apoptosis of differentiating spermatogonia. Alternatively, DND1 may associate with some proteins other than NANOS family proteins in differentiating spermatogonia, and play a role in the survival of these cells. To reveal the physiological function of DND1 in spermatogonia in more detail, loss-of-function analyses of DND1 should be conducted in either NANOS2-negative undifferentiated spermatogonia or differentiating spermatogonia. Lastly, it should be noted that we cannot rule out a possibility that a small number of cells in some somatic tissues express DND1, even if the present western blot analyses indicated DND1 expression only in the testis of 5-week-old mice. Therefore, a ubiquitous deletion of *Dnd1* might alter such tissues, which in turn would affect the maintenance of spermatogonia *via* mechanisms such as those involving the endocrine system. A detailed identification of DND1-expressing cells in somatic tissues and a specific deletion of *Dnd1* in such cells are required for further analyses of the physiological function of DND1.

In our analyses, we used mouse lines backcrossed to the MCH strain (Fig. 4N), and the portion of A_s in 5-week-old control mice was higher than those described in C57/BL6 or close to C57/BL6 (Choi et al., 2010; DeFalco et al., 2015; Gassei and Orwig, 2013; Nakagawa et al., 2010; Tokuda et al., 2007). Therefore, the different ratios of undifferentiated spermatogonial clusters might result from the genetic background. To clarify this point, we have counted the cluster number of undifferentiated spermatogonia in C57/BL6J mice in the same manner as Fig. 4N, and then calculated the portion of each cluster (Fig. S6). These analyses resulted in a data consistent with the previous assessments confirming that our experimental system is reliable, which in turn supports our notion that the higher portion of A_s is due to the mouse strain used in our experiments. If so, we cannot exclude a possibility that different ratio could be observed in *Dnd1*-cKO mice on other genetic backgrounds.

We showed that NANOS2 co-precipitated with DND1 from testis extracts and *vice versa*; to our knowledge, these data represent the first *in vivo* evidence of the interaction between NANOS2 and DND1 in spermatogonia. As NANOS2 interacts with the CCR4-NOT (CNOT) deadenylase complex (Fig. 5B), it is presumed that DND1 is required for loading specific RNAs into NANOS2-CNOT complex for suppression of the RNAs in spermatogonia as well as in male embryonic germ cells (Suzuki et al., 2009). However, the present antibody against NANOS2 was not suitable for analysis of the interaction of NANOS2 with RNAs by immunoprecipitation using testis extracts. This may be because the expression of NANOS2 is too low for the biochemical analysis, as NANOS2 is expressed only in a small population of

undifferentiated spermatogonia. A comprehensive identification of NANOS2-interacting RNAs in the presence and absence of DND1 is required for the elucidation of the biochemical function of DND1.

Recently, Photoactivatable ribonucleoside–enhanced crosslinking and immunoprecipitation (PAR-CLIP) analyses indicated that DND1 preferentially interacts with the sequences UUU or UUA in the 3′ UTR of target mRNAs in cultured cells, and the number of these consensus sequences controls the extent of DND1-mediated mRNA degradation (Yamaji et al., 2017). Therefore, we counted the sequences in the mRNAs, and found 8 sequences in *Sohlh1*, 31 in *Sohlh2*, 41 in *Dmrt1*, 96 in *Dazl*, 24 in *Taf7l*, and 34 in *Ddx4* mRNA (Fig. S7). However, the signal intensity in the RT-qPCR analyses, in which only *Dmrt1* mRNA was strongly detected, was not correlated with the numbers of these sequences (Fig. 5H). This might be because DND1 interacts with *Sohlh1*, *Sohlh2*, *Dazl*, and *Taf7l* mRNAs only in complex with NANOS2, whereas DND1 might associate with *Dmrt1* mRNA *via* not only NANOS2, but also other mechanisms. On the other hand, it is difficult to explain why neither DND1 nor NANOS2 associated with *Ddx4* mRNA, despite the fact that *Ddx4* mRNA has 34 consensus sequences in its 3′ UTR. We assume that a germ cell-specific mechanism might prevent DND1 from binding to *Ddx4* mRNA, and that such a mechanism does not exist in cultured cells. Alternatively, IP and RT-qPCR analyses might not be able to reflect the *in vivo* status of the interaction between DND1 and the target mRNAs as precisely as PAR-CLIP analysis. It is essential to comprehensively identify DND1-binding proteins and RNAs in germ cells for further understanding of DND1-mediated RNA metabolism *in vivo*.

Acknowledgements

We thank H. T. Timmers, T. Tamura, T. Hirata, H. Okayama, T. Iwamori and A. Rajkovic for gifting antibodies. We also thank T. Ichijo, Y. Odani, Y. Tazu, and Y. Hagiwara for technical assistance. This work was supported by the Japan Society for the Promotion of Science (KAKENHI Grant nos. 16H01252, 17H05046, 26114505, and 26440120) to A. Suzuki, and (KAKENHI Grant nos. 26251025 and 25112002) to Y. Saga.

Summary statement

DND1, which acts co-operatively with NANOS2 in male embryonic germ cells, plays an essential role for the maintenance of both undifferentiated spermatogonia and differentiating spermatogonia.

Appendix A. Supplementary material

Supplementary data associated with this article can be found in the online version at doi:10.1016/j.ydbio.2018.11.003.

References

Bhandari, D., Raisch, T., Weichenrieder, O., Jonas, S., Izaurralde, E., 2014. Structural basis for the Nanos-mediated recruitment of the CCR4-NOT complex and translational repression. Genes Dev. 28, 888–901.
Buaas, F.W., Kirsh, A.L., Sharma, M., McLean, D.J., Morris, J.L., Griswold, M.D., de Rooij, D.G., Braun, R.E., 2004. Plzf is required in adult male germ cells for stem cell self-renewal. Nat. Genet. 36, 647–652.
Chan, A.L., La, H.M., Legrand, J.M.D., Makela, J.A., Eichenlaub, M., De Seram, M., Ramialison, M., Hobbs, R.M., 2017. Germline stem cell activity is sustained by SALL4-dependent silencing of distinct tumor suppressor genes. Stem Cell Rep. 9, 956–971.
Choi, Y.H., Park, C.H., Kim, W., Ling, H., Kang, A., Chang, M.W., Im, S.K., Jeong, H.W., Kong, Y.Y., Kim, K.T., 2010. Vaccinia-related kinase 1 is required for the maintenance of undifferentiated spermatogonia in mouse male germ cells. PLoS One 5, e15254.
Costoya, J.A., Hobbs, R.M., Barna, M., Cattoretti, G., Manova, K., Sukhwani, M., Orwig, K.E., Wolgemuth, D.J., Pandolfi, P.P., 2004. Essential role of Plzf in maintenance of spermatogonial stem cells. Nat. Genet. 36, 653–659.
de Rooij, D.G., 1998. Stem cells in the testis. Int. J. Exp. Pathol. 79, 67–80.
de Rooij, D.G., 2001. Proliferation and differentiation of spermatogonial stem cells. Reproduction 121, 347–354.
de Rooij, D.G., 2017. The nature and dynamics of spermatogonial stem cells. Development 144, 3022–3030.
DeFalco, T., Potter, S.J., Williams, A.V., Waller, B., Kan, M.J., Capel, B., 2015. Macrophages contribute to the spermatogonial niche in the adult testis. Cell Rep. 12, 1107–1119.
Gassei, K., Orwig, K.E., 2013. SALL4 expression in gonocytes and spermatogonial clones of postnatal mouse testes. PLoS One 8, e53976.
Grasso, M., Fuso, A., Dovere, L., de Rooij, D.G., Stefanini, M., Boitani, C., Vicini, E., 2012. Distribution of GFRA1-expressing spermatogonia in adult mouse testis. Reproduction 143, 325–332.
Iwamori, N., Iwamori, T., Matzuk, M.M., 2012. Characterization of spermatogonial stem cells lacking intercellular bridges and genetic replacement of a mutation in spermatogonial stem cells. PLoS One 7, e38914.
Nakagawa, T., Sharma, M., Nabeshima, Y., Braun, R.E., Yoshida, S., 2010. Functional hierarchy and reversibility within the murine spermatogenic stem cell compartment. Science 328, 62–67.
Noguchi, T., Noguchi, M., 1985. A recessive mutation (ter) causing germ cell deficiency and a high incidence of congenital testicular teratomas in 129/Sv-ter mice. J. Natl. Cancer Inst. 75, 385–392.
Oatley, M.J., Kaucher, A.V., Racicot, K.E., Oatley, J.M., 2011. Inhibitor of DNA binding 4 is expressed selectively by single spermatogonia in the male germline and regulates the self-renewal of spermatogonial stem cells in mice. Biol. Reprod. 85, 347–356.
Sada, A., Suzuki, A., Suzuki, H., Saga, Y., 2009. The RNA-binding protein NANOS2 is required to maintain murine spermatogonial stem cells. Science 325, 1394–1398.
Schrans-Stassen, B.H., van de Kant, H.J., de Rooij, D.G., van Pelt, A.M., 1999. Differential expression of c-kit in mouse undifferentiated and differentiating type A spermatogonia. Endocrinology 140, 5894–5900.
Stevens, L.C., 1967. Origin of testicular teratomas from primordial germ cells in mice. J. Natl. Cancer Inst. 38, 549–552.
Stevens, L.C., 1973. A new inbred subline of mice (129-terSv) with a high incidence of spontaneous congenital testicular teratomas. J. Natl. Cancer Inst. 50, 235–242.
Suzuki, A., Igarashi, K., Aisaki, K., Kanno, J., Saga, Y., 2010. NANOS2 interacts with the CCR4-NOT deadenylation complex and leads to suppression of specific RNAs. Proc. Natl. Acad. Sci. USA 107, 3594–3599.
Suzuki, A., Niimi, Y., Shinmyozu, K., Zhou, Z., Kiso, M., Saga, Y., 2016. Dead end1 is an essential partner of NANOS2 for selective binding of target RNAs in male germ cell development. EMBO Rep. 17, 37–46.
Suzuki, A., Saga, Y., 2008. Nanos2 suppresses meiosis and promotes male germ cell differentiation. Genes Dev. 22, 430–435.
Suzuki, H., Ahn, H.W., Chu, T., Bowden, W., Gassei, K., Orwig, K., Rajkovic, A., 2012. SOHLH1 and SOHLH2 coordinate spermatogonial differentiation. Dev. Biol. 361, 301–312.
Suzuki, H., Sada, A., Yoshida, S., Saga, Y., 2009. The heterogeneity of spermatogonia is revealed by their topology and expression of marker proteins including the germ cell-specific proteins Nanos2 and Nanos3. Dev. Biol. 336, 222–231.
Suzuki, H., Tsuda, M., Kiso, M., Saga, Y., 2008. Nanos3 maintains the germ cell lineage in the mouse by suppressing both Bax-dependent and -independent apoptotic pathways. Dev. Biol. 318, 133–142.
Tokuda, M., Kadokawa, Y., Kurahashi, H., Marunouchi, T., 2007. CDH1 is a specific marker for undifferentiated spermatogonia in mouse testes. Biol. Reprod. 76, 130–141.
Weidinger, G., Stebler, J., Slanchev, K., Dumstrei, K., Wise, C., Lovell-Badge, R., Thisse, C., Thisse, B., Raz, E., 2003. dead end, a novel vertebrate germ plasm component, is required for zebrafish primordial germ cell migration and survival. Curr. Biol. 13, 1429–1434.
Yamaji, M., Jishage, M., Meyer, C., Suryawanshi, H., Der, E., Yamaji, M., Garzia, A., Morozov, P., Manickavel, S., McFarland, H.L., Roeder, R.G., Hafner, M., Tuschl, T., 2017. DND1 maintains germline stem cells via recruitment of the CCR4-NOT complex to target mRNAs. Nature 543, 568–572.
Yamatani, H., Sato, Y., Fujisawa, H., Hirata, T., 2004. Chronotopic organization of olfactory bulb axons in the lateral olfactory tract. J. Comp. Neurol. 475, 247–260.
Yoshida, S., Takakura, A., Ohbo, K., Abe, K., Wakabayashi, J., Yamamoto, M., Suda, T., Nabeshima, Y., 2004. Neurogenin3 delineates the earliest stages of spermatogenesis in the mouse testis. Dev. Biol. 269, 447–458.
Yoshinaga, K., Nishikawa, S., Ogawa, M., Hayashi, S., Kunisada, T., Fujimoto, T., Nishikawa, S., 1991. Role of c-kit in mouse spermatogenesis: identification of spermatogonia as a specific site of c-kit expression and function. Development 113, 689–699.
Youngren, K.K., Coveney, D., Peng, X., Bhattacharya, C., Schmidt, L.S., Nickerson, M.L., Lamb, B.T., Deng, J.M., Behringer, R.R., Capel, B., Rubin, E.M., Nadeau, J.H., Matin, A., 2005. The Ter mutation in the dead end gene causes germ cell loss and testicular germ cell tumours. Nature 435, 360–364.
Zheng, K., Wu, X., Kaestner, K.H., Wang, P.J., 2009. The pluripotency factor LIN28 marks undifferentiated spermatogonia in mouse. BMC Dev. Biol. 9, 38.
Zhou, Z., Shirakawa, T., Ohbo, K., Sada, A., Wu, Q., Hasegawa, K., Saba, R., Saga, Y., 2015. RNA binding protein Nanos2 organizes post-transcriptional buffering system to retain primitive state of mouse spermatogonial stem cells. Dev. Cell 34, 96–107.